

UNDER-DENSITY REGIONS AND THE PRIMORDIAL DENSITY FIELD

KIM, MINSUN AND PARK, CHANGBOM

Department of Astronomy, Seoul National University, Seoul, 151-742, Korea

mskim@astro.snu.ac.kr

cbp@astro.snu.ac.kr

(Received Sep. 10, 1998; Accepted Oct. 8, 1998)

ABSTRACT

We show that the low density regions of the matter distribution preserve the properties of the primordial density field better than the high density regions. We have performed a cosmological N-body simulation of large-scale structure formation in the standard CDM cosmology, and studied the evolution of statistics of under-density and over-density regions separately. The rank-order of the under-density regions is closer to the original one compared to that of the over-density regions. The under-density peaks (or voids) has moved less than over-density peaks (or dense clusters of galaxies) from their initial positions. Therefore, the under-density regions are more useful than the over-density regions in the study of the statistical property of the primordial density field.

Key Words : cosmology: theory - primordial density field: statistical properties, under-density region - method: numerical

I. INTRODUCTION

The primordial density field contains information on the mechanism for generation of the density fluctuation in the early universe and on the nature of the dark matter. Therefore, it is important to measure the physical properties of the primordial density field to constrain cosmological models. This is not easy because the relation between the primordial and the present density fields is not linear due to the non-linear gravitational evolution and the biased structure formation.

The primordial density field is often assumed to be a Gaussian random field. Bardeen *et al.* (1986) have presented the statistical properties of peaks in the Gaussian random field. At the present epoch, the statistical properties of high density peaks are significantly changed due to non-linear gravitational evolution (Sugimoto & Suto 1991).

There have been many attempts to relate the primordial density field with the present one. Using the Zel'dovich approximation, the present potential field has been evolved backward in time and estimated the primordial density or velocity field (Nusser & Dekel 1992; Croft & Gaztañaga 1997). The Gaussianization method assumes a Gaussian primordial density field and performs one-to-one mapping of the present density field to the primordial density field using rank-order of the density field (Weinberg 1992). The cosmological statistics method is to find out the form of transformation between the linear and non-linear correlation functions or power spectra of the density fluctuations from N-body simulations. Statistics at the primordial epoch are estimated from the observed ones at the present epoch using the transformation formula (Hamilton *et al.* 1991; Peacock & Dodds 1994; Jain *et al.* 1995; Baugh & Gaztañaga 1996). Croft & Gaztañaga (1998) have studied the spectral param-

eters of the peak number density in Gaussian density fields, and estimated the index of the primordial power spectrum.

Properties of the primordial density field have also been studied observationally. Piran *et al.* (1993) have used a simple model for the gravitational formation of voids, and compared the results with the matter fluctuations as constrained by the CMBR observations of COBE. They have found a power spectrum $P(k) \propto k^n$ with $n \approx 1.25$. Little & Weinberg (1994) have performed cosmological N-body simulations and found that the void probability function (VPF) can distinguish unbiased models from some biased models. They have calculated the VPF from the observed data and concluded that there is no strong biasing. Nusser *et al.* (1995) have recovered the one-point probability distribution function of the initial density fluctuations from the quasi-linear density field of the 1.2Jy IRAS redshift survey smoothed over $10 h^{-1} \text{Mpc}$. From this one-point probability distribution function of the initial density fluctuations, they have found that the initial density field is consistent with a Gaussian.

Most previous studies have utilized the whole density field or the high density peaks to explore the properties of the primordial field. In this paper we show that the under-density region of the gravitationally evolved density field better preserves the statistical properties of the primordial density field. A cosmological N-body simulation is used to demonstrate that the relation between under-dense regions of the present and the primordial density fields is better than that between dense regions.

In section II, we describe our cosmological N-body simulation and the gravitational evolution of the density field. In section III, we compare the statistical properties of over- and under-density regions. Discus-

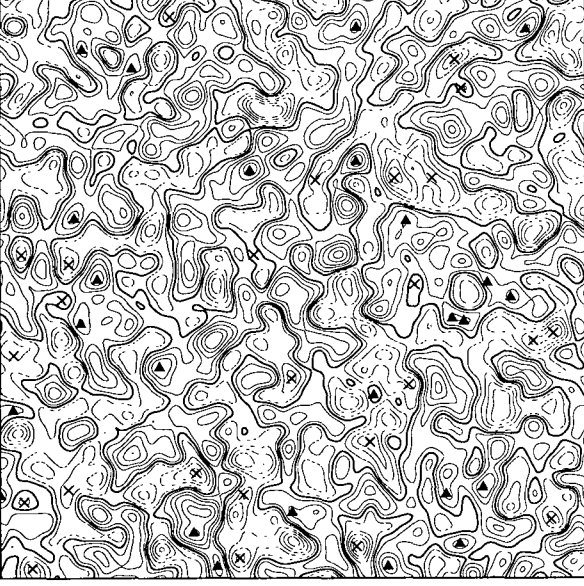
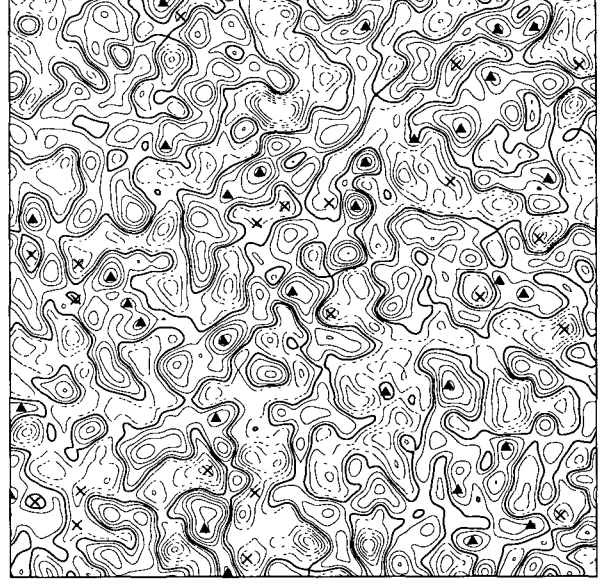
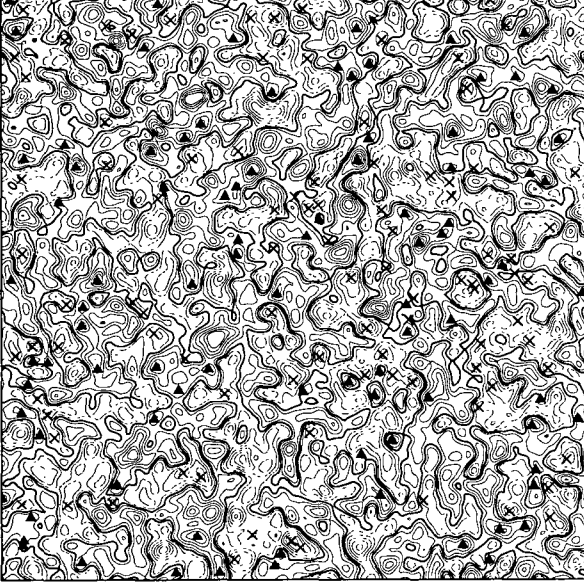
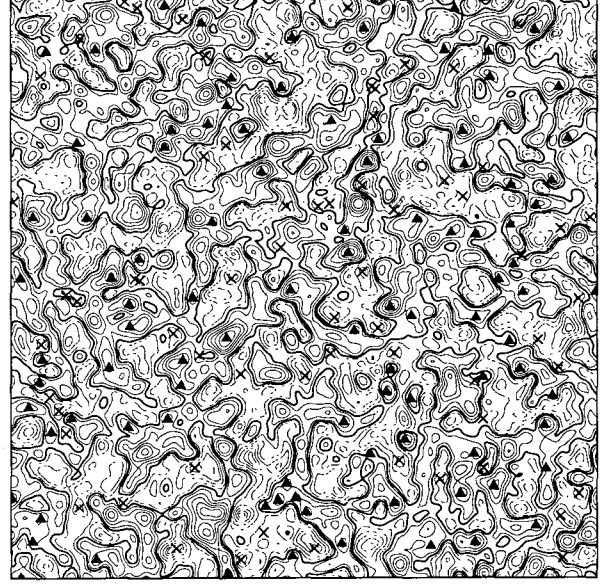
(a) $\lambda=8h^{-1}\text{Mpc}$ ($z=23$)(b) $\lambda=8h^{-1}\text{Mpc}$ ($z=0$)(c) $\lambda=5h^{-1}\text{Mpc}$ ($z=23$)(d) $\lambda=5h^{-1}\text{Mpc}$ ($z=0$)

Fig. 1.— Density fields in a slice at $z = 23$ (left panels) and 0 (right panels). The length of the slice is $614.4h^{-1}\text{Mpc}$ along a side. Particle distributions are smoothed with the Gaussian filter over 8 (upper panels) and $5h^{-1}\text{Mpc}$ (lower panels). The heavy solid lines are the mean density contours. The under-density (dashed lines) and the over-density (thin solid lines) contours are spaced at 0.5 intervals in unit of the volume fraction label (see the text). Triangles represent over-density peaks and crosses are under-density peaks.

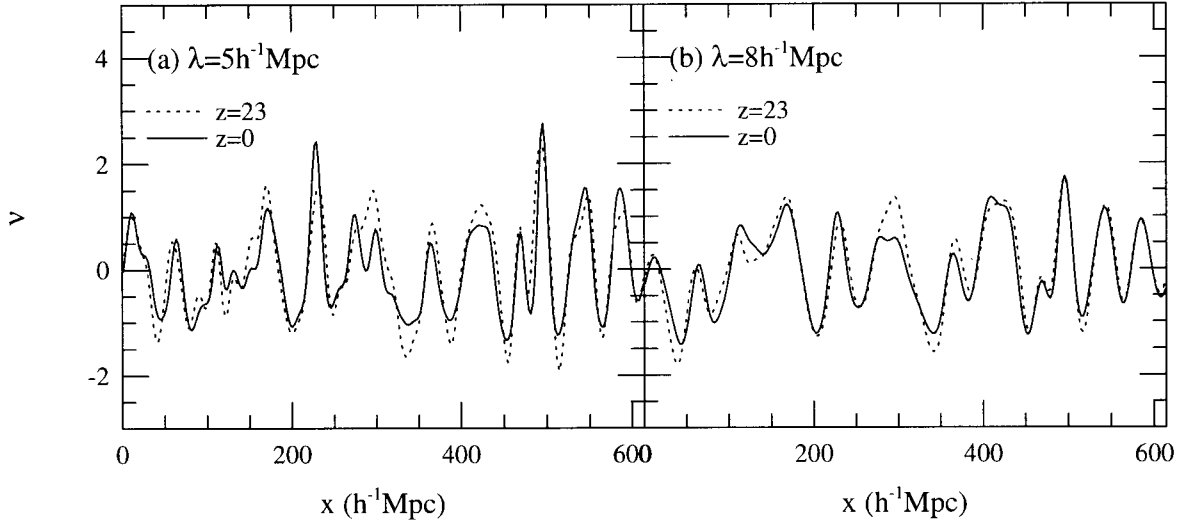


Fig. 2.— The profiles of density fluctuation at $z = 23$ and 0 along a random line in the simulation cube. Density field has been smoothed over (a) $5h^{-1}\text{Mpc}$ and (b) $8h^{-1}\text{Mpc}$. The dashed line is for $z = 23$ and the solid line is for $z = 0$.

sion and conclusions follow in section IV.

II. GRAVITATIONAL EVOLUTION OF UNDER- AND OVER- DENSITY REGIONS

We have performed a cosmological N-body simulation to study the gravitational evolution of over- and under-density regions. We have adopted the standard Cold Dark Matter model with $\Omega_0 = 1$ and $h = 0.5$. Choice of a specific model would not affect our results. The simulation was run by a PM code (Park 1997), and 256^3 particles were moved in a 512^3 mesh with physical size of $614.4h^{-1}\text{Mpc}$ along a side, and with periodic boundary conditions. The simulation was started at $z = 23$ and made 115 steps to reach the present.

We have calculated the density at 256^3 grid points using the TSC (Triangular-Shaped-Cloud) scheme (Hockney & Eastwood 1988). This mass assignment scheme yields smoother and more accurate representation of particle distribution compared to the CIC (Cloud-in-Cell) scheme. Density fields at different epochs are smoothed by Gaussian filters with radii of 5 and $8h^{-1}\text{Mpc}$. Melott(1993) has claimed that a sharp truncation of the power spectrum leads to a more direct connection to initial conditions for either the Gaussianization method or the Zel'dovich approximation method. However, we used the Gaussian filter because it is simple and conventional. We have searched for local density extremes whose densities are higher (or lower) than those of the nearest 26 cells. Then the locations of the centers of peaks are found by fitting the Gaussian ball.

Figure 1 shows the density fields in a typical slice smoothed over $8h^{-1}\text{Mpc}$ (a and b) and $5h^{-1}\text{Mpc}$ (c and d) at $z = 23$ (a and c) and $z = 0$ (b and d). Heavy solid lines are the mean density contours. Under-density

(dashed line) and over-density (light solid line) contours are spaced at 0.5 intervals in unit of the volume fraction label (see section III below). Also shown in Figure 1 are the positions of peaks. Triangles represent the centers of over-density peaks, and crosses are at under-density peaks. It will be shown that the initial positions of peaks and shapes of contours are kept better in under-density regions.

Figure 2 compares the initial ($z = 23$) and the final ($z = 0$) density fields along a line chosen randomly. The density fluctuation is shown in unit of $\nu(\vec{x}) = (\rho(\vec{x}) - \bar{\rho})/\sigma$. Here, ρ is the local density, $\bar{\rho}$ is the mean density, and σ is the standard deviation of the smoothed density field. Despite the gravitational evolution, there is significant correlation between the density fields at $z = 23$ and 0 at these smoothing scales. However, there are differences in the density profiles at small scales. In the next section, evolution of the under- and over-density regions will be compared.

III. STATISTICAL PROPERTIES OF UNDER- AND OVER- DENSITY REGIONS

To investigate the statistical properties of under-density and over-density regions, we have assigned the volume fraction index to 256^3 grid points corresponding to the local density. For a Gaussian density field, the volume fraction f_v is a function of the number of standard deviations ν_v (Vogeley *et al.* 1994),

$$f_v = (2\pi)^{-1/2} \int_{\nu_v}^{\infty} e^{-x^2/2} dx. \quad (1)$$

For the more general case of a non-Gaussian density distribution, this relation does not hold. Non-linear

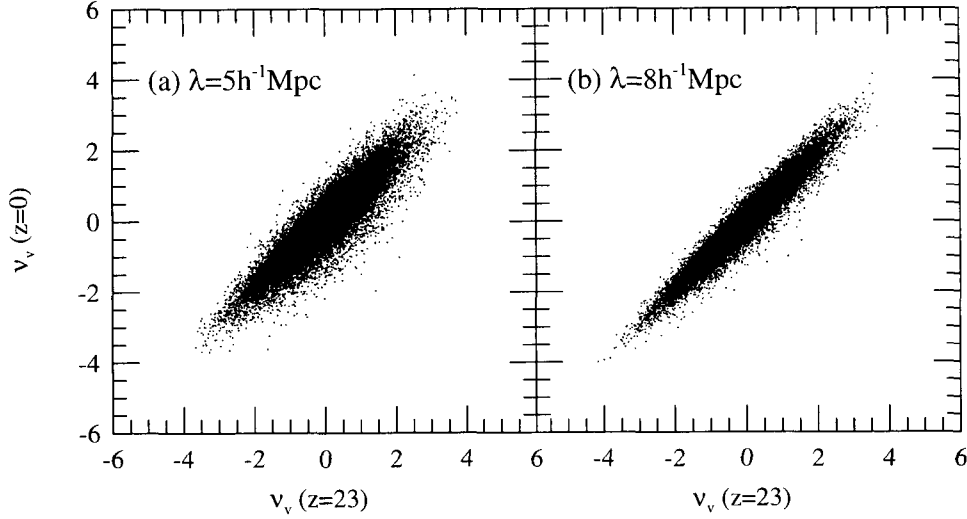


Fig. 3.— The rank-order correlations of the volume fraction index ν_v between the initial ($z = 23$) and final ($z = 0$) density fields smoothed over (a) $5h^{-1}\text{Mpc}$ and (b) $8h^{-1}\text{Mpc}$. Only the density at every eight pixel along each side of the simulation cube is plotted. The rank of under-density regions is kept better than that of over-density regions.

evolution skews the probability distribution of the field, generating the high density tail. In the case of a non-Gaussian field we calculate f_v at each grid point corresponding to the density at that pixel. For example, the pixel with the highest density has the volume fraction of $1/256^3$. We then assign the label ν_v to the pixel corresponding to f_v using equation (1).

We compare the label ν_v at each pixel at two epochs $z = 0$ and 23 . We call this relation the “rank-order correlation”. Figure 3 shows the rank-order correlation of the density field smoothed over $5h^{-1}\text{Mpc}$ (hereafter DS5V) and $8h^{-1}\text{Mpc}$ (DS8V). Only the density at every eight pixel along each side is used. The low density tail is narrower than the high density tail, making the correlation tighter at under-dense regions. But at high density regions, the correlation is weaker for higher threshold levels. The relation for DS8V is tighter than that for DS5V because DS8V is more linear.

We have measured the displacement of density peaks from their initial positions due to the gravitational evolution. We match the peaks found at different epochs in space instead of tracing them in time. The *rms* displacement of matter in the comoving space at time t can be derived as follows (Park & Gott 1991);

$$\langle |\Delta x|^2 \rangle_m^{1/2} = \int_0^t \left\langle \left| \frac{dx}{dt} \right|^2 \right\rangle^{1/2} dt = \left[\int \frac{d^3k}{(2\pi)^3} \frac{P(k, t)}{k^2} \right]^{1/2}. \quad (2)$$

But above equation overestimates the *rms* displacement because the matter stops travelling when it forms pancakes in the non-linear regime. We use this *rms* displacement as a constraint of match between the peaks found at two different epochs. For example, the peak found at $z = 23$ nearest to and located within 1.5

$\langle |\Delta x|^2 \rangle_m^{1/2}$ from a peak found at $z = 0$, is identified as the pair at its initial location.

After matching the peaks, we have calculated the match rate of peaks by the following formula:

$$\text{match rate} = \frac{\text{number of matched peaks}}{\text{total number of primordial peaks}}. \quad (3)$$

Figure 4a and 4b show the match rates of peaks in DS5V and DS8V, respectively, as a function of ν_v . Circles are for over-density peaks, and crosses for under-density peaks. In DS5V the match rate for under-density peaks is higher than that of over-density peaks for peaks with $|\nu_v| > 0.8$. This is also true for peaks with $|\nu_v| > 1.2$ in DS8V.

Figure 5 shows the rank-order correlation of peaks matched between the epochs $z = 23$ and 0 . It can be seen that at high threshold levels the correlation between under-density peaks is clearly stronger than that between over-density peaks. The variance of the relation is smaller for under-density peaks at $|\nu_v| \gtrsim 2$.

We introduce the *rms* displacement of matched peaks

$$\langle |\Delta x|^2 \rangle^{1/2} = \left[\sum_{i=1}^N (\vec{x}_{\text{initial}}(i) - \vec{x}_{\text{final}}(i))^2 / N \right]^{1/2}, \quad (4)$$

where N is the total number of the matched peaks, and the initial and final epochs correspond to $z = 23$ and 0 , respectively. Figure 6 shows that the *rms* displacement of the under-density peaks from their initial positions is smaller than that of over-density peaks. These results indicate that under-density peaks better preserve the statistical properties of the primordial density field than over-density peaks.

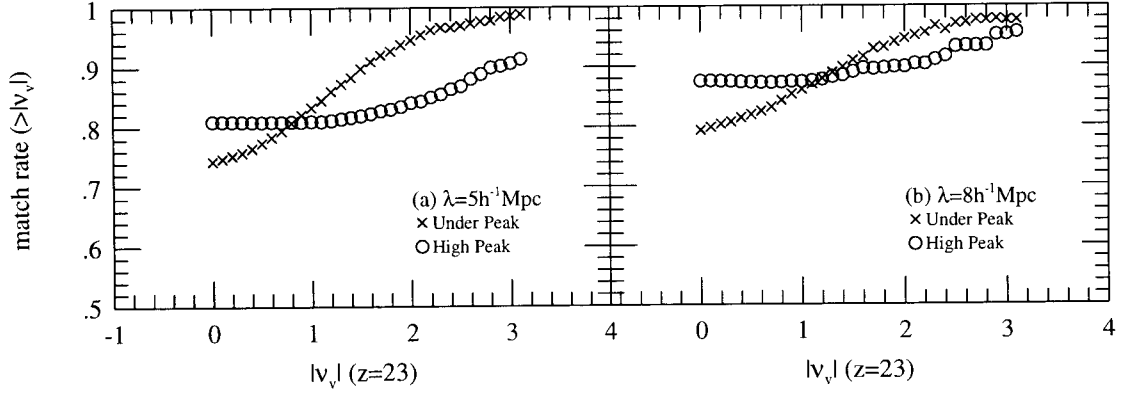


Fig. 4.— The match rates between the peaks found at $z = 23$ and 0. Crosses are for the under-density peaks, and circles for the over-density peaks. The x -axis is the absolute value of the volume fraction index at $z = 23$.

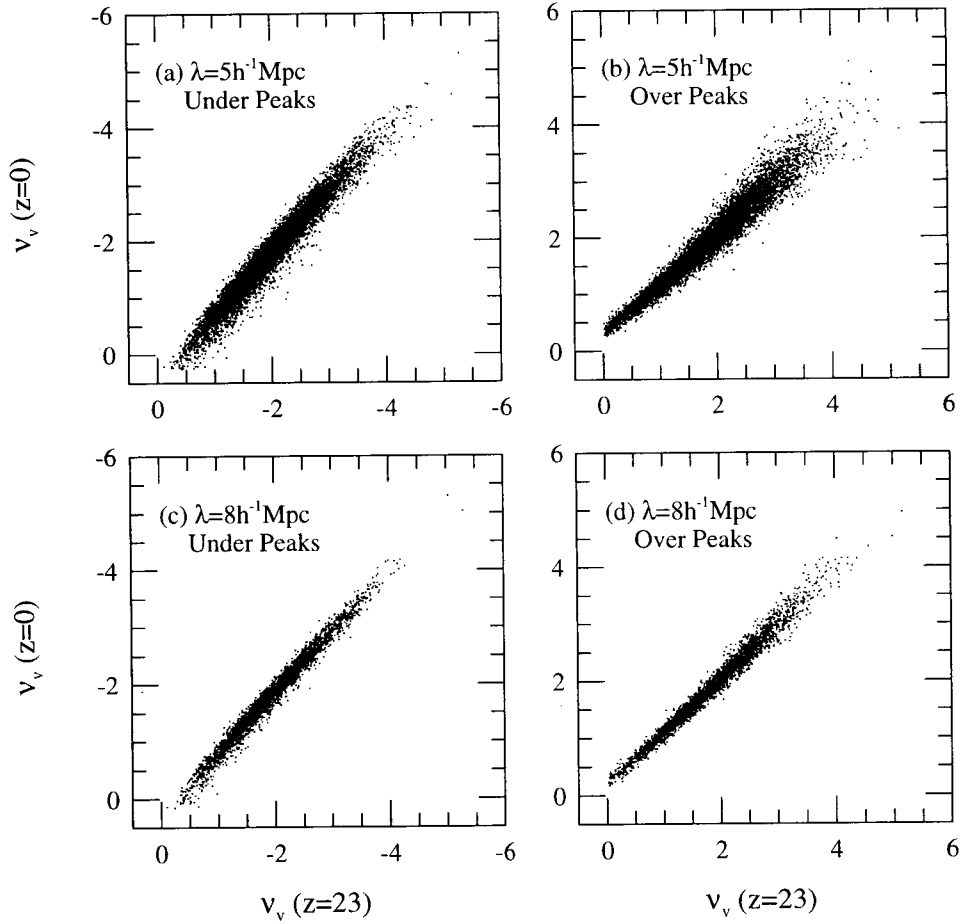


Fig. 5.— The correlations of rank-orders between matched peaks found at $z = 23$ and at 0. The upper panels are for the peaks in the density field smoothed over $5h^{-1}\text{Mpc}$ and the lower panels are for $8h^{-1}\text{Mpc}$ smoothing. The left panels are for the under-density peaks and the right panels for the over-density peaks. Correlations between over-density peaks are weaker than those between under-density peaks at high threshold levels.

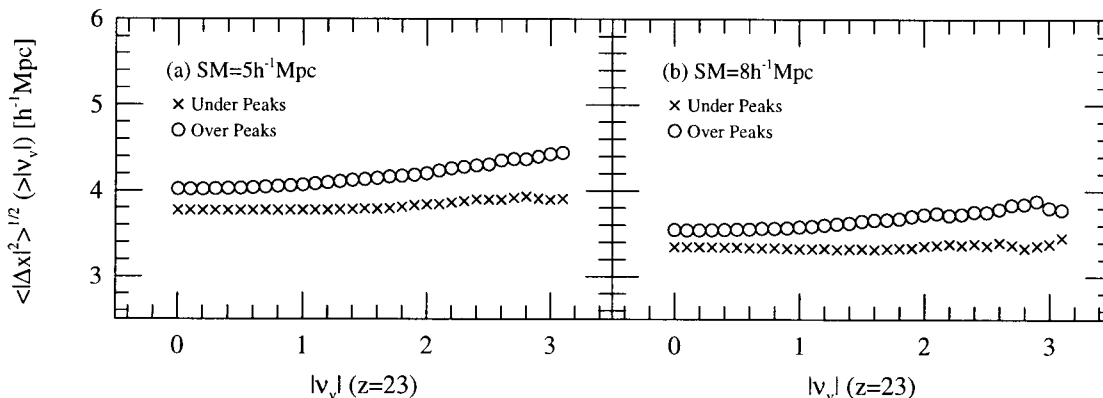


Fig. 6.— The rms displacements of peaks in the density fields smoothed over $5h^{-1}\text{Mpc}$ (left panel) and $8h^{-1}\text{Mpc}$ (right panel). Circles are for over-density peaks and crosses are for under-density peaks. The x -axis is the volume fraction label assigned to the peaks found at $z = 23$.

IV. DISCUSSION AND CONCLUSION

We have studied the statistical properties of the under- and over-density regions in smoothed density fields. We have found that the properties of the primordial density field are better preserved in the under-density regions than in the over-density regions. The rank-order correlation between the primordial and the evolved density fields are higher in under-density regions than in over-density regions. The *rms* displacement of under-density peaks (or center of voids) from their initial positions is smaller than that of over-density peaks (or dense clusters of galaxies). Therefore, we can constrain cosmological models more strongly by using the properties of under-density regions. One practical problem is that voids are harder to identify than clusters of galaxies. The survey has to be large and dense enough to locate many voids accurately.

Mo *et al.* (1996) have determined the cosmic density parameter Ω_0 and the amplitude of mass fluctuations σ_8 by using large redshift survey catalogs of galaxies and galaxy clusters. They have suggested that if a cluster sample is complete above some mass threshold, hierarchical theories for structure formation predicts its autocorrelation function, which is entirely determined by the cluster abundance and by the spectrum of linear density fluctuations. Thus, if the shape of the initial fluctuation spectrum is known, its amplitude σ_8 can be estimated directly from the correlation length of a cluster sample. Although there exist some problems in observing voids, if we can use empty voids, instead of dense clusters, we can calculate Ω_0 and σ_8 more accurately.

Sahni *et al.* (1994) have applied the adhesion approximation to study the formation and evolution of voids and found a strong correlation between the size of voids and the value of the primordial gravitational potential at void centers. Their study could provide a

way of reconstructing the form of the primordial potential from the observed void spectrum. However, it is uncertain whether this relation is true or not on the non-linear state of the density field due to gravitational evolution. In addition, there are various definitions for voids and different algorithms to identify them (Vetolani *et al.* 1985; Pellegrini *et al.* 1989; Einasto *et al.* 1989; Kauffmann & Fairall 1991; Slezak *et al.* 1993; Ryden & Melott 1996; El-Ad & Piran 1997). Therefore, the relation between the size of voids and the value of the primordial gravitational potential at void centers depends on these definitions and algorithms.

In the present study we have shown that the under-density region preserves information on the primordial density field better than the over-density region by directly comparing the density fields at the initial and the present epochs. In the future study we will compare various statistics extracted from the under- and over-density regions to demonstrate that the under-density region is more useful in exploring the properties of the primordial density field.

ACKNOWLEDGEMENTS

This work was supported by '96 S.N.U. Daewoo Research Fund.

REFERENCES

- Bardeen, J. M., Bond, J. R., Kaiser, N., & Szalay, A. S. 1986, ApJ, 304, 15
- Baugh, C. M., & Gaztañaga, G. 1996, MNRAS, 280, L37
- Croft, R. A. C., & Gaztañaga, E. 1997, MNRAS, 285, 793
- Croft, R. A. C., & Gaztañaga, E. 1998, ApJ, 495, 554
- Einasto, J., Einasto, M., & Gramann, M. 1989, MNRAS, 238, 155
- El-Ad, H., & Piran, T. 1997, ApJ, 491, 421

- Hamilton, A. J. S., Kumar, P., Lu, E., & Matthews, A. 1991, *ApJ*, 374, L1
- Hockney, R. W., & Eastwood, J. W. 1987, *Computer Simulation Using Particles*, Adam Hilger, New York
- Jain, B., Mo, H. J., & White, S. D. M. 1995, *MNRAS*, 276, L25
- Kauffmann, G., & Fairall, A. P. 1991, *MNRAS*, 248, 313
- Little, B., & Weinberg, D. H. 1994, *MNRAS*, 267, 605
- Melott, A. 1993, *ApJ*, 414, L73
- Mo, H. J., Jing, Y. P., & White, S. D. M. 1996, *MNRAS*, 282, 1096
- Nusser, A., & Dekel, A. 1992, *ApJ*, 391, 443
- Nusser, A., Dekel, A., & Yahil, A. 1995, *ApJ*, 449, 439
- Park, C., & Gott, J. R. 1991, *MNRAS*, 249, 288
- Park, C. 1997, *J. Kor. Astron. Soc.*, 30, 191
- Peacock, J. A., & Dodds, S. J. 1994, *MNRAS*, 267, 1020
- Pellegrini, P. S., da Costa, L. N., & de Carvalho, R. R. 1989, *ApJ*, 339, 595
- Piran, T., Lecar, M., Goldwirth, D. S., da Costa, L. N., & Blumenthal, G. R. 1993, *MNRAS*, 265, 681
- Ryden, B. S., & Melott, A. L. 1996, *ApJ*, 470, 160
- Sahni, V., Sathyaprakash, B. S., & Shandarin, S. F. 1994, *ApJ*, 431, 20
- Slezak, E., de Lapparent, V., & Bijaoui, A. 1993, *ApJ*, 409, 517
- Suginohara, T., & Suto, Y. 1991, *ApJ*, 371, 470
- Vogeley, M. S., Park, C., Geller, M. J., Huchra, J. P., & Gott, J. R. 1994, *ApJ*, 420, 525
- Vettolani, G., de Souza, R. E., Marano, B., & Chincarini, G. 1985, *A&A*, 144, 506
- Weinberg, D. H. 1992, *MNRAS*, 254, 315